Electrospray–Differential Mobility Analysis as an Orthogonal Tool to Size-Exclusion Chromatography for Characterization of Protein Aggregates

SUVAJYOTI GUHA,[1,2] JOSHUA R. WAYMENT,[1] MICHAEL J. TARLOV,[1] MICHAEL R. ZACHARIAH[1,2]

[1]National Institute of Standards and Technology, Gaithersburg, Maryland 20899

[2]Departments of Mechanical Engineering, Chemistry and Biochemistry, University of Maryland, College Park, Maryland 20742

Received 26 September 2011; revised 11 January 2012; accepted 9 February 2012

Published online 12 March 2012 in Wiley Online Library (wileyonlinelibrary.com). DOI 10.1002/jps.23097

ABSTRACT: The biopharmaceutical industry characterizes and quantifies aggregation of protein therapeutics using multiple analytical techniques to cross-validate results. Here, we demonstrate the use of electrospray–differential mobility analysis (ES–DMA), a gas-phase and atmospheric pressure ion-mobility method for characterizing protein aggregates. Two immunoglobulin Gs are systematically heat treated to induce aggregation and characterized using size-exclusion chromatography (SEC) and ES–DMA. Although ES–DMA is a gas-phase characterization method, we find that aggregation kinetic rate constants determined by ES–DMA is in good agreement with those determined by SEC. ES–DMA appears to have a higher resolution and lower limit of detection as compared with SEC. Thus, ES–DMA can potentially become an important orthogonal tool for characterization of nascent protein aggregates in the biopharmaceutical industry. © 2012 Wiley Periodicals, Inc. and the American Pharmacists Association J Pharm Sci 101:1985–1994, 2012

Keywords: immunoglobulins; electrospray–differential mobility analysis; size-exclusion chromatography; protein formulation; protein aggregation; biopharmaceutics; physical characterization; protein size; biotechnology; stability

INTRODUCTION

Detection and characterization of protein aggregates in formulations is of prime importance to the biopharmaceutical industry.[1–3] A concentration–size chart summarizing the most commonly used methods for sizing aggregates is presented in Figure 1.[4,5]

Because protein aggregates span a wide range of sizes and quantification of aggregates depends on the technique employed, there is no analytical tool that can measure all classes of aggregates,[6–8] and multiple methods are typically used for cross-validation.[4,6,9] The objective of this paper is to evaluate electrospray–differential mobility analysis (ES–DMA) as another method to add to the suite of protein aggregate characterization tools.

Differential mobility analysis has been used extensively in the aerosol field, but has been only recently applied to the characterization of proteins.[10–14] Because the DMA is a gas-phase electrophoretic or ion-mobility device, ES is used in a manner analogous to that employed in mass spectrometry to generate aerosol-phase protein. At low concentrations of analyte in solution, ES and subsequent evaporation of volatile solvent leaves behind one analyte per parent droplet (either single protein or oligomers). If particles (in our case proteins) are charged, their size can be measured directly by DMA, which acts as a narrow-band-pass ion-mobility filter. More detailed descriptions of the theoretical and operational details of DMA can be found elsewhere.[15,16]

Our current configuration of the ES–DMA can characterize particles from approximately 3 nm[14] up to approximately 150 nm spherical equivalent diameters.[17] From prior work it has been determined that the lower limit of detection of ES–DMA is in picomolar range.[11,13,18–20] Although the upper limit of concentration, till recently, had been limited by the inability to differentiate between intrinsic aggregates

Additional Supporting Information may be found in the online version of this article. Supporting Information

Correspondence to: Michael R. Zachariah (Telephone: +301-405-4311; Fax: +301-405-4311; E-mail: mrz@umd.edu)

Journal of Pharmaceutical Sciences, Vol. 101, 1985–1994 (2012)

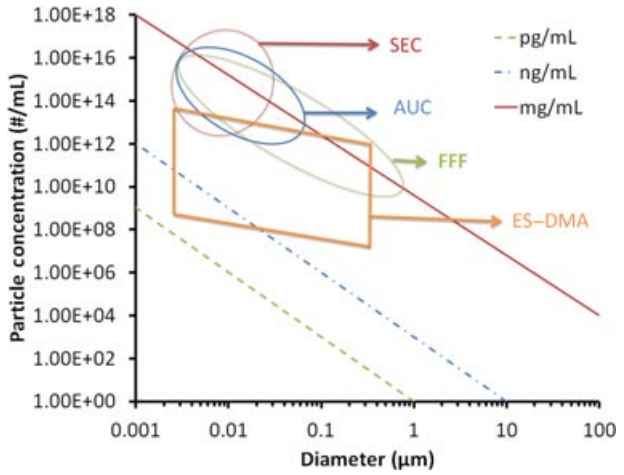

Figure 1. The concentration and size landscape of the most popular characterization tools—namely, size-exclusion chromatography (SEC), analytical ultracentrifugation (AUC), and field-flow fractionation (FFF).[5] The solid and dashed lines represent boundaries for constant mass of protein particles, assuming a spherical density of 1 gm/cc. This figure also shows the landscape of electrospray–differential mobility analysis (ES–DMA). A detailed discussion of ES–DMA appears in the text.

from aggregates formed from different oligomers residing in the same ES droplet,[11,21] we have recently developed a method[21] that corrects for this effect, which we will employ in this study. As shown by Figure 1, ES–DMA, size-exclusion chromatography (SEC), analytical ultracentrifugation (AUC), and field-flow fractionation overlap in the range of analyte sizes they characterize. However, ES–DMA offers a limit of detection that is at least two orders of magnitude lower.

In this study, we compare SEC with ES–DMA using two proteins, a monoclonal antibody therapeutic of the immunoglobulin G1 (IgG1) class, Rituxamab®(RmAb), and a polyclonal human antibody [human-derived IgG (hIgG)]. The proteins are systematically heat stressed to promote the formation of aggregates, which is characterized using both techniques.

MATERIALS AND METHODS

Protein Sample Preparation

Rituxamab® (Genentech, CA) was purified using protein A affinity column and stored at–18°C in 25 mmol/L Tris buffer at pH 7.4, to which 1×10^{-5} mol/L of NaN_3 was added as a preservative. To desalt the protein sample, a centrifuge filter [30 kDa molecular weight (MW) cutoff] was used immediately prior to ES–DMA analysis at 13,200 rpm for 12 min. The concentration of RmAb in 20 mmol/L ammonium acetate at pH 7 was diluted to 1 mg/mL, as verified by ultraviolet–visible (UV–Vis) spectrometer (Lamda Bio 20, PerkinElmer,Waltham, MA)). Further details are provided elsewhere.[21]

The hIgG (# I4506; Sigma–Aldrich, St. Louis, Missouri) was prepared by suspending 1–1.5 mg in 1–1.5 mL of buffer (20 mmol/L ammonium acetate at pH 7 in low-protein-binding vials).

All samples were diluted to concentrations of about 0.1 mg/mL in 20 mmol/L ammonium acetate buffer at pH 7 for analysis with ES–DMA and SEC. This diluted concentration was not verified by UV–Vis spectrometer, as it was below the limit of quantitation of our instrument. Samples that were not heat treated were used as controls. Aggregate formation was accelerated by subjecting samples to 70°C for 30, 60, 90, and 120 min for RmAb and for 10, 20, 30, 60, 90, and 120 min for IgG to monitor the time evolution of the aggregate formation. The heat-incubated samples were preserved in the refrigerator at 4°C before analysis. Because the heat-treated samples showed evidence of large aggregates that could potentially clog up ES capillaries and size-exclusion columns, we filtered the samples using 0.22-μm filters (Millex GV, catalog #SLGV004SL; Millipore, Billerica, MA) prior to characterization.

Size-Exclusion Chromatography

Size-exclusion chromatography was performed with an Agilent 1200 system using a TSK 3000 gel-filtration column at ambient temperature (Agilent Technologies, Santa Clara, CA). Using 20 mmol/L ammonium acetate buffer in the SEC column caused the IgGs to adsorb to the SEC column, and no protein would elute for several hours. Thus, 100 mmol/L potassium phosphate at pH 7 along with 300 mmol/L sodium chloride was used as reported in other studies.[22,23] The injection volume was 50 μL at 0.5 mL/min flow rate, with UV detection at 280 nm. Because the concentration of the protein injected and recovered were below the limit of quantitation of our UV–Vis spectrometer, the recovery could not be calculated for hIgG and RmAb. However, several steps were taken that qualitatively suggested that protein adsorption (especially the monomers) to the SEC column was low. Before running the actual heat-treated samples for analysis, the columns were pretreated with heat-incubated samples ($t = 30$ min sample for hIgG and $t = 60$ min for RmAb) three times (approximately 30 min each). SEC chromatograms obtained for these samples did not show any difference from run to run. Further, after finishing all experiments for the day, the column would be flushed with buffer (100 mmol/L potassium phosphate at pH 7 along with 300 mmol/L sodium chloride) for 1.5 h followed by a 10% methanol wash, during which only nominal

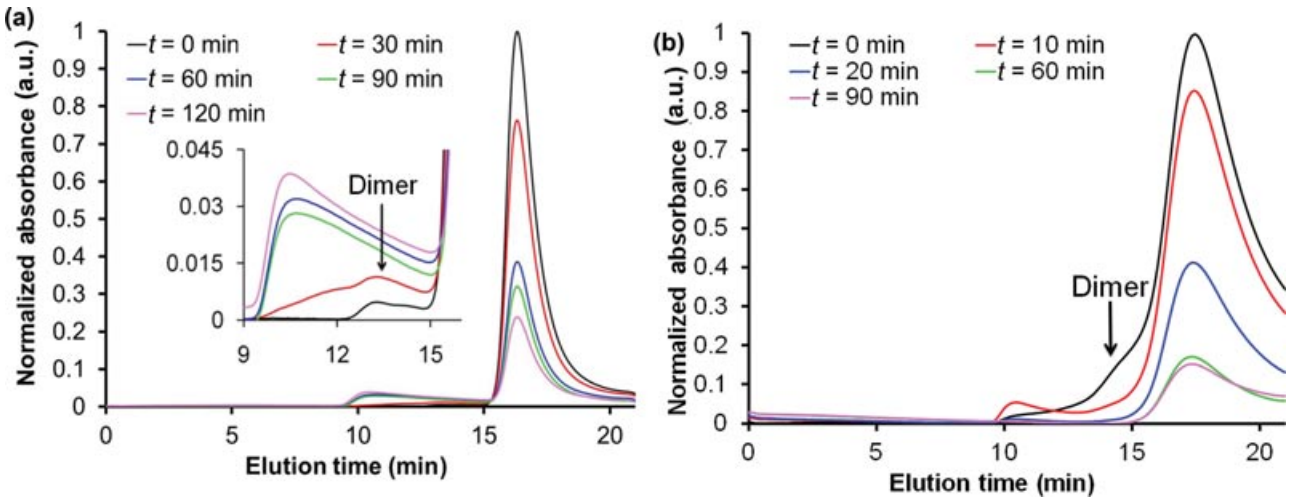

Figure 2. (a) Chromatograms of Rituxamab® obtained with size-exclusion chromatography (SEC) for heat-treated samples at increasing incubation times at 70°C. The inset shows a magnification of the aggregate region. (b) Chromatograms of human-derived immunoglobulin G obtained with the SEC for heat-treated samples at different incubation times at 70°C. For both panels a and b, the normalization has been carried out with respect to the area under the monomer peak at $t = 0$ min.

protein would desorb from the column, implying nominal adsorption to the column. For quantitative analysis, it is also assumed that the recovery of monomers at different incubation times stay the same for the proteins.

The dimers and monomers were quantified by integrating from elution times of 14.33–20.81 min and 11.62–14.32 min, respectively. The fractional percentages of dimers were determined by first integrating the area under the monomer and dimer peaks at that particular incubation time, and then dividing dimer peak area by the monomer peak area at the same incubation time. The background noise for the SEC was determined by integrating the area under the monomer and dimer peaks after running 20 mmol/L ammonium acetate buffer in triplicates. The respective average values obtained were 534 and 222 arbitrary units (a.u.). In Figure 2, for both RmAb and hIgG, the acetate peak elutes first (before 20 min) in all samples and has not been shown for clarity.

Electrospray–Differential Mobility Analysis

Figure 3 depicts our ES–DMA system, which consists of an ES aerosol generator (model 3480; TSI Inc., Shoreview, MN), a Po-210 radiation source (also called a neutralizer), a differential mobility electrode column (model 3080; TSI Inc.), and a condensation particle counter (CPC, model 3025; TSI Inc.). The ES was operated with a 25 μm diameter, 24 cm long, silica-coated capillary (TSI, Inc.) The liquid delivery rate and the droplet size generated were controlled by changing the ES chamber pressure. To operate in the "Taylor cone mode," chamber pressures of 3.0 and 3.7 PSI were used, for which the size of the monodispersed droplets generated was 120.4 and 138.1 nm, respectively. These droplet sizes were determined using an approach discussed elsewhere.[21] Briefly, a 20 mmol/L ammonium acetate buffer at pH 7 was prepared with a known concentration of sucrose (0.063%, v/v) and electrosprayed. Because sucrose is nonvolatile, as the ES droplet evaporated, a residue of sucrose was left. This residue size was measured with our DMA, which was then used to extract the ES droplet size based on a correlation between the

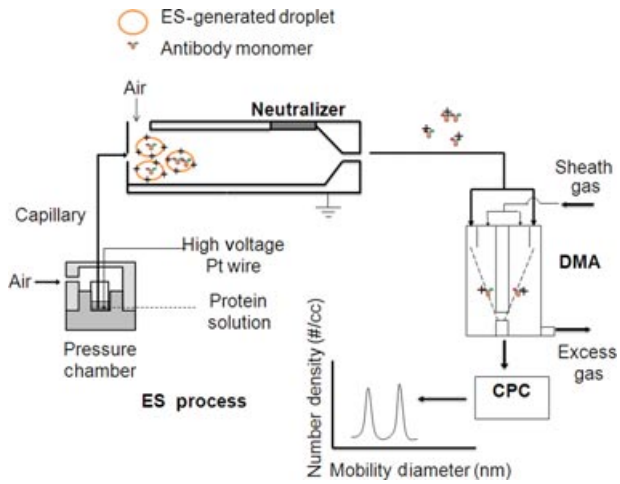

Figure 3. Electrospray–differential mobility analysis (ES–DMA) system consisting of an ES charge neutralizer to produce aerosolized, singly charged protein particles; a differential mobility analyzer to separate them by their charge-to-size ratio; and a condensation particle counter to enumerate the size-selected proteins.

ES droplet size and residue size for a known liquid-phase concentration of the nonvolatile sucrose.[24]

Air as the carrier gas (also referred to as aerosol flow) was introduced at 1.2 L/min, and the aerosol stream was passed through a radioactive Po-210 source, which reduced the highly charged analytes to primarily 0, +1, or–1 charges.[25,26] The +1-charged dry particles were separated within the differential mobility analyzer on the basis of their electrical mobility by applying a negative voltage. Although only the +1-charged particles were collected, the total particle count could be deduced because the proportions of all the charges were known.[25] The CPC was operated at a "high-flow mode[17]" such that the CPC flow rate was 1.5 L/min. The system was calibrated for size with 60-nm polystyrene latex beads (National Institute of Standards and Technology SRM 1963). The flow rate in the ES capillary was approximately 66 nL/min. The voltage and current measured in the ES unit were approximately in between 1.6 and 1.8 kV and −170 and −180 nA, respectively, for all samples.

The resolution in the DMA[27] is determined by the ratio of the input aerosol flow to the DMA clean carrier gas flow (also known as the sheath flow). To achieve sufficient resolution from the DMA, the ratio of sheath-to-aerosol flow rates within the DMA was set to 25, which provides a theoretical resolution of approximately 0.4 nm for the antibodies. Under these conditions, data were collected with a voltage scanning step size of 0.2 nm and a dwell time of 10 s from 2 to 45 nm—that is, it would take approximately 36 min to obtain each ES–DMA size distribution, comparable to SEC experiment. However, commercial softwares (Aerosol Instrument Manager; TSI Inc.) can be used to obtain ES–DMA size distributions in a matter of few minutes (2–4 min), as has been demonstrated elsewhere.[10] Thus, ES–DMA analysis time can be shorter as compared with that of SEC.

From the size distribution (number concentration vs. size), the area under the monomer, dimer, trimer, tetramer, and pentamer peaks were determined by integrating from 7.8 to 9.8, 10.0 to 11.6, 11.8 to 13.0, 13.2 to 13.8, and 14.0 to 14.8 nm, respectively. Oligomers were identified by an empirical correlation between mobility diameter and MW, which is discussed in greater detail in *Results and Discussion*. The average background noise in ES–DMA under the monomer, dimer, trimer, tetramer, and pentamer peaks was found to be 241, 125, 54, 23, and 18 particles/cm^3, respectively.

About 20–30 μL aliquots of samples were for used for analysis, but only 2–3 μL was consumed during the course of an experiment—that is, the sample volume requirement of ES–DMA is significantly less as compared with that of SEC.

The reader should note that the signal produced by the ES–DMA can be material dependent. For example, we have found that the signal produced by gold nanoparticles and viruses are more compared with that of proteins.[14,20] Similar observations have been made by the mass spectrometry community.[28] However, we have also found that despite the material dependency, ES–DMA size distributions (after correcting for ES artifacts) can reflect the intrinsic levels of aggregates of different particles in solution or, in other words, ES–DMA can be used for determining absolute liquid-phase concentrations irrespective of material property.[21,29]

Passivation of ES Capillary

We have found that different IgGs tend to adsorb to the capillary walls of the ES capillaries, which is problematic because it leads to a time-variant size distribution and may affect quantification of different oligomers,[30] but can be significantly reduced by passivating the capillaries with gelatin. Prior to ES of protein samples, 0.5–1.0 mol/L H_2SO_4, deionized (18 MΩ/cm) ultrapure water, and 20 mmol/L ammonium actetate buffer solutions were eluted sequentially for 20–30 min through 25-μm fused silica capillaries (TSI Inc.). Subsequently, 0.1 mg/mL gelatin (trade name: Knox Gelatine, Krafts Food Inc., catalog #0-41000-03500-5, Fairfax, VA) prepared in 20 mmol/L ammonium acetate buffer at pH 7 was electrosprayed through the capillary for about 1 h, followed by 20 mmol/L ammonium actetate buffer for 10 min. We have found that this protocol results in significantly (approximately 93%–95%) reduction of RmAb and IgG monomer adsorption.[31] Curiously, we also found that for heat-treated samples of RmAb, the intrinsic tetramers, pentamers, and larger aggregates would show a propensity to adsorb to this passivated surface for approximately 1 h. In such cases, before quantifying these aggregates, we would wait till the size distribution of the aggregates had become invariant of time, at which point we would assume that the adsorption of these aggregates were minimal. We also compared size distributions of RmAb and IgG obtained on bare capillary surface after steady state with size distributions obtained on passivated surfaces to conclude that the gelatin passivation had no effect on the original size distributions.

RESULTS AND DISCUSSION

Size Distributions Obtained with ES–DMA

Figure 4a shows the size distributions of the RmAb obtained by ES–DMA for unstressed ($t = 0$ min) sample and samples that were incubated at 70°C for increasing incubation times. For peak identification, we used the correlation from Bacher et al.[10] between mobility

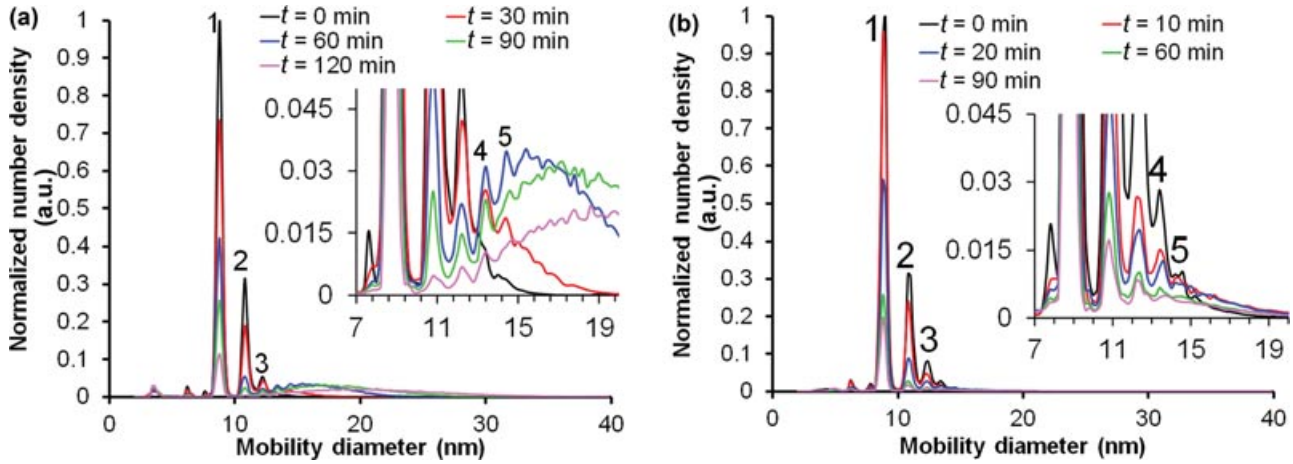

Figure 4. (a) Size distribution of Rituxamab® for increasing incubation times at 70°C. The inset shows a magnification of different aggregates as a function of the incubation time. (b) Size distribution of immunoglobulin G prepared at different incubation times at 70°C. The inset does not show any evidence of increasing tetramers, pentamers, and other higher-order oligomers. In both panels a and b, data are normalized in terms of the monomer peaks at $t = 0$ min. The peaks labeled 1, 2, 3, 4, and 5 refer to the monomers, dimers, trimers, tetramers, and pentamers, respectively. For both panels a and b, the normalization has been carried out with respect to the area under the monomer peak at $t = 0$ min. All distributions are at an electrospray capillary pressure drop of 3.7 PSI. Size distributions obtained at 3.0 PSI pressure have not been shown, but show similar trend.

size (d) and MW expressed in kDa:

$$\mathrm{MW} = -22.033 + 9.83d - 1.247d^2 + 0.228d^3 \qquad (1)$$

Using this correlation, the monomer, dimer, trimer, tetramer, and pentamer peaks for IgG with a MW of 150 kDa should appear at 9.3, 11.7, 13.4, 14.7, and 15.8 nm, respectively. This correlation was specific to their experimental setup and operating conditions, and can vary up to 1 nm for different DMAs.[32] We find the monomer, dimer, trimer, tetramer, and pentamer peaks to appear at 8.8, 10.8, 12.6, 13.4, and 14.4 nm, respectively, in reasonable agreement with the predicted values. Pease et al.[13] have also shown that the sizes of IgG oligomers as measured by the ES–DMA are in excellent agreement with the structural dimensions obtained from protein crystallographic database. Thus, oligomer peaks from ES–DMA size distributions can be identified with a high degree of confidence. Besides these, there are three peaks that are characterized at sizes 3.6, 6.2, and 7.6 nm. The proportion of these peaks are insignificant ($\ll$1%) as compared with all other peaks, and correspond to the nonvolatile solute, which may be still present in the solution after the desalting step; doubly charged monomers of RmAb (not intrinsic to the solution, produced during neutralization in the gas phase); and dimers of Fab fragments of RmAb, respectively.

The size distributions in Figure 4a show a decreasing trend for monomers (labeled 1), dimers (labeled 2), and trimers (labeled 3) with increasing incubation time, whereas the tetramers (labeled 4) and pentamers (labeled 5) increase initially (t = 30 and 60 min, respectively), but subsequently decrease at later times. Although larger oligomers are clearly evident in the spectra, the resolution is insufficient to make a definitive assignment. The maximum intensity of the aggregates for the sample incubated for 120 min appear at mobility diameter of 19–20 nm. Assuming the correlation of Bacher et al.,[10] the MW at this mobility diameter corresponds to approximately 1300–1500 kDa—that is, the most of these aggregates are probably enneamers (nine-mers) and decamers (10-mers) of RmAb.

Figure 4b shows the size distributions for hIgG, where the oligomers are again identified using the correlation of Bacher et al.[10] Like RmAb, the monomers (labeled 1), dimers (labeled 2), and trimers (labeled 3) decrease with incubation; however, unlike RmAb, the larger aggregates do not increase with the incubation time. The size distribution also shows two smaller peaks ($\ll$1% compared with other peaks) at 6.2 and 7.8 nm, which correspond to the doubly charged monomers (not intrinsic to the solution, produced during neutralization in the gas phase) and dimers of Fab fragments, respectively. It is possible that larger aggregates of RmAb and hIgG (>50 nm) form with increasing incubation time at concentrations below the limit of detection of ES–DMA. In fact, at longer incubation times, visible precipitation was observed for both proteins. Flow imaging methods indicated increasing concentrations of particulates

with the incubation time, ranging in size from 4 to 100 μm for both RmAb and hIgG, respectively (data not shown).

A complicating factor in using ES–DMA for protein aggregation measurements is that when the proteins (or any particle to be analyzed) in solution are volatilized by ES, two monomers of the protein residing in the same droplet will appear as dimers in the ES–DMA spectrum. This artifact, which we refer to as "droplet-induced aggregation," depends on the droplet volume and the concentration of the protein in solution with increasing protein concentration or increasing droplet volume, worsening this ES artifact.[11] However, we have recently developed a statistical model that quantitatively describes this bias and allows for its compensation.[21] The application of this model also allows ES–DMA analysis of higher concentration samples, and improved detection and quantification of large aggregates. For example, working at limits of concentration for ES–DMA previously reported in the literature,[10–12] it would have been difficult to detect the tetramers, pentamers, and larger aggregates of RmAb, as seen in Figure 4a, because they would be close to the detection limit of the ES–DMA.

For simplicity, we assume that only monomers and dimers exist in the solution. This is a reasonable assumption based on previous findings using other aggregate-characterization techniques[21–23] and by using SEC, as discussed in the next section, for IgG and RmAb. In all such cases, the proportion of the intrinsic trimers was negligible (<1%).

With this assumption, it can be shown that [21]

$$\frac{N_{o2}}{N_{o1}} = \frac{\overline{V_{d_1}} C_{p1}}{2} + \frac{C_{p2}}{C_{p1}} \tag{2}$$

where N_{02} and N_{01} are experimentally observed dimers and monomers obtained by integrating the area under the dimer and monomer peaks; $\overline{V_{d_1}}$ is the corresponding droplet volume obtained in a separate experiment with the ES–DMA (data not shown), and its unit is expressed in m^3; and C_{p1} and C_{p2} are the intrinsic, that is, actual, concentrations of monomers and dimers in solution, which can be determined such that the total concentration of the protein, C_p, would be given by the summation of C_{p1} and twice C_{p2}. Here, the units of C_{p1} and C_{p2} are expressed in particles/m^3. Similarly, changing the ES capillary pressure and thus generating another droplet volume $\overline{V_{d_2}}$,we can obtain

$$\frac{N'_{o2}}{N'_{o1}} = \frac{\overline{V_{d_2}} C_{p1}}{2} + \frac{C_{p2}}{C_{p1}} \tag{3}$$

where N_{02}' and N_{01}' are experimentally determined monomers and dimers at a different capillary pressure drop, for which the experimentally determined droplet volume is $\overline{V_{d_2}}$.

Solving Eqs. 2 and 3 simultaneously, we can obtain the intrinsic monomer (C_{p1}) and dimer (C_{p2}) concentrations in solution. The percentage of the intrinsic dimers determined following this approach is discussed later.

The larger aggregates, as measured by the ES–DMA, are quantified and plotted as a percentage of all oligomers present at each incubation time in the supporting information (Fig. S1). It is evident that for RmAb, the proportion of tetramers and larger oligomers increases as a function of incubation time (supporting information Fig. S1A), whereas for IgG, the proportion remains constant (supporting information Fig. S1B).

SEC Chromatograms

Figure 2a shows SEC chromatograms of RmAb for increasing incubation times at 70°C. In SEC, larger aggregates will elute first, and so the last peak is assigned to the monomer. We see little evidence of dimers and trimers in the $t = 0$ and 30 min samples. Larger aggregates appear after $t = 60$ min, which increase in intensity with the incubation time. Figure 2b shows SEC chromatograms of hIgG. The mode of the monomer peak for both RmAb and hIgG are at approximately 16.3 min, but the full width at half maximum for hIgG is approximately 5.43 min as compared with only approximately 1.38 min for RmAb, implying that hIgG interacts with the SEC column longer. Evidence for larger aggregates are observed for short incubation periods, but drop below the background after 10 min of incubation. The fact that the monomer peak is dropping, with no observation of higher aggregates at long incubation times, would indicate that larger oligomers grow very rapidly, depleting the system of intermediates (dimers, trimers, etc.).

Comparison of ES–DMA with SEC

Table 1 compares the dimer proportions obtained by SEC and ES–DMA (before and after correcting for "droplet-induced aggregates") for RmAb and hIgG. For columns 2, 4, 5, and 7 of Table 1, the dimer to monomer proportions have been determined by dividing the area under the dimer peaks with the area under the monomer peaks at that incubation time. For columns 3 and 6, the dimer to monomer ratio represents C_{p2}/C_{p1} determined after solving Eqs. 2 and 3 simultaneously. It is evident from the ES–DMA results that a major proportion of the dimers detected are droplet induced, consistent with our previous findings.[21] Even after correction for "droplet-induced aggregates," we find that ES–DMA indicates a higher fraction of dimers than SEC at $t = 0$ min. In order to understand the possible sources for the discrepancy in between these two techniques, we also

Table 1. Dimer to Monomer Ratio for ES–DMA Before and After Correcting for "Droplet-Induced Aggregates" and SEC at Different Incubation Times at 70°C

	RmAb			hIgG		
Time (min)	ES–DMA Before Correction Dimer (%)	ES–DMA After Correction Dimer (%)	SEC Dimer (%)	ES–DMA Before Correction Dimer (%)	ES–DMA After Correction Dimer (%)	SEC Dimer (%)
0	33.0 ± 2.0	5.0 ± 2.0	1.0 ± 0.4	37.0 ± 5.0	12.0 ± 6.0	7.0 ± 2.0
10	–	–	–	25.0 ± 1.0	7.0 ± 2.0	4.0 ± 2.0
20	–	–	–	18.0 ± 2.0	7.0 ± 2.0	ND[a]
30	27.0 ± 2.0	5.0 ± 2.0	2.0 ± 0.1	16.0 ± 2.0	8.0 ± 4.0	ND[a]
60	15.0 ± 1.0	2.0 ± 1.0	ND[b]	13.0 ± 2.0	7.0 ± 2.0	ND[a]
90	11.0 ± 2.0	3.0 ± 2.0	ND[b]	11.0 ± 1.0	6.0 ± 2.0	ND[a]
120	6.0 ± 1.0	2.0 ± 1.0	ND[b]	9.0 ± 2.0	4.0 ± 2.0	ND[a]

The standard error bars are calculated from measurements on three samples.
[a]The signal-to-noise ratio for the dimers for these samples were less than 3.
[b]For these samples, the SEC was not able to resolve the dimers from the larger aggregates and hence the dimers were not quantified.
ND, not determined.

quantified the dimer to monomer proportions using AUC for the $t = 0$ min samples; the dimer to monomer ratio for RmAb and hIgG were determined to be 4.8 ± 0.8% and 11.7 ± 1.9%, respectively (supporting information Fig. S2). Thus, the dimer to monomer ratio obtained using AUC and ES–DMA appear to be the same and slightly greater than that by SEC. Out of the three techniques, the error bars in the dimer percentage measurement of ES–DMA is the highest, perhaps because of the variability in the measurement of ES droplet sizes. We were unable to quantify the percentage of the dimers and larger oligomers for the heat-incubated samples using AUC, as the dimer and other oligomer proportions in these samples were below the limit of detection of the AUC, but, as evident from Table 1, for all heat-incubated samples, the dimer to monomer proportion obtained with ES–DMA was greater than that by SEC (except hIgG at $t = 0$ min, for which the dimer to monomer proportion obtained with ES–DMA and SEC were comparable). We can speculate that there are several possible reasons for these differences. Firstly, both in ES–DMA and SEC, protein is subject to shear forces, which could potentially induce aggregation or alternatively break small oligomers apart. Secondly, high salt concentrations in the mobile phase of the SEC are used to minimize the adsorption of protein, but it is known that high salt concentrations can also break up aggregates.[9] Thirdly, prior work by others has indicated that dimers may preferentially absorb in the SEC column.[8,33] Inaccuracies can also arise in determining the dimer to monomer ratio using ES–DMA. There could be two sources for this: (a) Eqs. 2 and 3 depend on the droplet volumes of the ES, and any inaccuracy in these measurements can propagate in the determination of the dimer to monomer ratio; and (b) for RmAb, we initially assume there are monomers and dimers in solution; however, with increasing incubation time (after 60 min), we find evidence of trimers, tetramers, and larger aggregates that are intrinsic to the solution, which we do not account for in our modeling.

On the basis of the signal to noise (S/N) ratio of the monomers and larger aggregates for the different samples obtained with SEC and ES–DMA, we can qualitatively compare the detection limits for these two methods. For ES–DMA, considering RmAb sample at $t = 120$ min, the monomer, dimer, trimer, tetramer, and pentamer average counts were 158,961 particles/cm^3 (not corrected for droplet-induced artifacts), 8371 particles/cm^3 (not corrected for droplet-induced artifacts), 13,467, 18,780, and 25,913 particles/cm^3, respectively. Comparing these values with the background noise (provided in *Materials and Methods*), it is evident that the S/N ratio was two to three orders of magnitude higher than the background noise. On the contrary, for the same sample, the average monomer counts obtained with SEC was 5342 a.u., and thus the monomer S/N ratio was approximately 10 (the background noise for SEC monomers is provided in *Materials and Methods*), whereas the S/N ratio for dimer was less than 3. Thus, ES–DMA appears to have a lower limit of detection.

Despite the differences in the dimer fractions, there appears to be good agreement in the relative amount of monomer decay between ES–DMA and SEC, as can be seen in the normalized monomer plots of RmAb (Fig. 5a) and hIgG (Fig. 5b) as a function of the incubation time. The reader is reminded that although the SEC is a relative measurement, the ES–DMA can provide an absolute concentration of monomer.[29]

The monomer decay can be described by a general rate equation:

$$\frac{dC}{dt} = -kC^n \tag{4}$$

where C is the concentration of the monomer in the liquid phase at time t, k is the rate constant, and n is the reaction order.

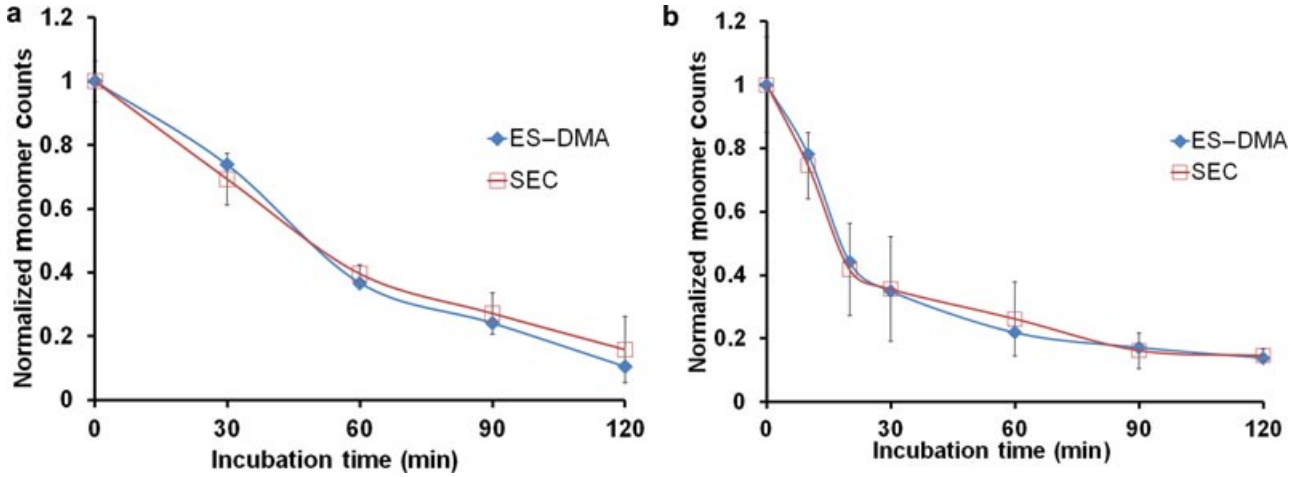

Figure 5. (a) Normalized monomer counts for Rituxamab® as a function of the incubation time at 70°C, obtained with size-exclusion chromatography (SEC) and electrospray–differential mobility analysis (ES–DMA; after correcting for "droplet-induced aggregation"). (b) Normalized monomer counts for human-derived immunoglobulin G as a function of the incubation time at 70°C, obtained with SEC and ES–DMA (after correcting for "droplet-induced aggregation"). The error bars are for measurements made in triplicate. For the SEC, normalization has been carried out with respect to the total area under the monomer peak at $t = 0$ min. For ES–DMA, the normalization has been carried out with respect to the absolute monomer concentration determined by solving Eqs. 2 and 3 simultaneously at $t = 0$ min.

For $n = 1$, assuming C_o is the initial monomer concentration, the concentration of monomers C_t at time t is

$$\mathrm{In}\left(\frac{C_t}{C_o}\right) = -kt \tag{5}$$

For $n \neq 1$, the general rate equation can be solved to get

$$\left(\frac{C_t}{C_o}\right)^{1-n} = 1 - (n-1)kC_o^{n-1}t \tag{6}$$

Further, $kC^{n-1}{}_o$can be replaced with an apparent rate constant k', such that

$$\left(\frac{C_t}{C_o}\right)^{1-n} = 1 - (n-1)k't \tag{7}$$

For IgGs, a wide range of reaction orders have been proposed: $n = 1.0$,[34,35] 1.2,[36] 1.5,[37,38] 2.0,[39,40] or 2.5.[41] The order of the reaction is typically determined by fitting the experimental data using different reaction orders and assigning the order with the highest R^2 value.

The reaction-order-fitting results are presented in Table 2. In the case of RmAb, we find that both ES–DMA and SEC indicate a reaction order of approximately unity. Physically, this may either imply that the aggregation process is unfolding limited or occurs via monomer addition to oligomers.[42] Despite being completely different techniques, the difference in the decay rate constants are within 5% of each other and in good agreement with those reported previously[40,43] for the temperature range 55°C–70°C.

Table 2. Rate Constants and R^2 Values Obtained for RmAb and IgG Using ES–DMA and SEC by Fitting Different Reaction Orders

	RmAb				hIgG			
	ES–DMA		SEC		ES–DMA		SEC	
n	k' (min^{-1})	R^2	k' (min^{-1})	R^2	k' (min^{-1})	R^2	k' (min^{-1})	R^2
1	0.0073[a]	0.97	0.0069[a]	0.99	0.0096	0.84	0.0083	0.84
1.2	0.0210	0.94	0.0175	0.98	0.0235	0.89	0.0230	0.90
1.5	0.0292	0.88	0.0226	0.96	0.0316	0.95	0.0304	0.97
2	0.0540	0.77	0.0364	0.88	0.0549[b]	0.99	0.0517[b]	0.99
2.5	0.1095	0.66	0.0625	0.79	0.1023	0.98	0.0939	0.96
3	0.2430	0.57	0.1137	0.71	0.2024	0.95	0.1809	0.91

[a] The uncertainty in the rate constant measurement for ES–DMA and SEC were determined to be ±0.001 and ±0.0016 min^{-1}, respectively, based on measurements on three samples.

[b] The uncertainty in the rate constant measurement for ES–DMA and SEC were determined to be ±0.003 and ±0.011 min^{-1}, respectively, based on measurements on three samples.

For hIgG, a second-order reaction yields the best fit for both SEC and ES–DMA. This physically implies that the rate of dimer formation is controlling the rate of monomer depletion. The apparent rate constant k' obtained for hIgG is in good agreement with the values obtained elsewhere[36,39,44] at 65°C–70°C. In addition, the rate constants obtained by both methods agree well, differing by only approximately 6%.

CONCLUSIONS

Using two heat-incubated IgGs, we have compared ES–DMA with SEC in their ability to characterize oligomers. Results of this study indicate that ES–DMA can be a useful method for monitoring protein stability and for characterizing protein aggregates, and its capabilites are at par and, in some cases (e.g., resolution and detection limit), better than those of SEC. ES–DMA observes a higher fraction of dimers, and because of its inherent higher resolving power and lower limit of detection, was able to characterize the larger oligomers that were not apparent in SEC at the concentrations used in this paper ($\leq$0.1 mg/mL). In addition, ES–DMA generally has shorter analysis time and lower sample volume requirements than SEC. ES–DMA, however, has certain limitations: the ES requires volatile buffers and a narrow range of ionic strengths (typically few mmol/L to 80 mmol/L),[13,16,45] suffers from artifacts,[11,21] and capillaries can become clogged for samples with significant soluble aggregates. In the future, to make ES–DMA acceptable as a process analytical tool, it would be perhaps useful to compare this technique against other "gold standard" methods such as AUC.

ACKNOWLEDGMENTS

The authors would like to thank Vinayak Rastogi and James Falabella for running experiments with analytical ultracentrifuge for protein samples. Suvajyoti Guha would like to thank Mingdong Li for helpful discussions during the experimentation phase. Certain commercial equipments, instruments, or materials are identified in this paper to specify the experimental procedure adequately. Such identification is not intended to imply that the materials or equipments identified are necesserily the best available for the purpose.

REFERENCES

1. Chi EY, Krishnan S, Randolph TW, Carpenter JF. 2003. Physical stability of proteins in aqueous solution: Mechanism and driving forces in nonnative protein aggregation. Pharm Res 20:1325–1336.
2. Fink AL. 1998. Protein aggregation: Folding aggregates, inclusion bodies and amyloid. Fold Des 3:R9–R23.
3. Rosenberg AS. 2006. Effects of protein aggregates: An immunologic perspective. AAPS J 8:E501–E507.
4. Mahler HC, Friess W, Grauschopf U, Kiese S. 2009. Protein aggregation: Pathways, induction factors and analysis. J Pharm Sci 98:2909–2934.
5. Singh SK, Afonina N, Awwad M, Bechtold-Peters K, Blue JT, Chou D, Cromwell M, Krause HJ, Mahler HC, Meyer BK, Narhi L, Nesta DP, Spitznagel T. 2010. An industry perspective on the monitoring of subvisible particles as a quality attribute for protein therapeutics. J Pharm Sci 99:3302–3321.
6. Carpenter JF, Randolph TW, Jiskoot W, Crommelin DJA, Middaugh CR, Winter G, Fan YX, Kirshner S, Verthelyi D, Kozlowski S, Clouse KA, Swann PG, Rosenberg A, Cherney B. 2009. Overlooking subvisible particles in therapeutic protein products: Gaps that may compromise product quality. J Pharm Sci 98:1201–1205.
7. Philo J. 2006. Is any measurement method optimal for all aggregate sizes and types? AAPS J 8:564–571.
8. Arakawa T, Ejima D, Li TS, Phil JS. 2010. The critical role of mobile phase composition in size exclusion chromatography of protein pharmaceuticals. J Pharm Sci 99:1674–1692.
9. Carpenter JF, Randolph TW, Jiskoot W, Crommelin DJA, Middaugh CR, Winter G. 2010. Potential inaccurate quantitation and sizing of protein aggregates by size exclusion chromatography: Essential need to use orthogonal methods to assure the quality of therapeutic protein products. J Pharm Sci 99:2200–2208.
10. Bacher G, Szymanski WW, Kaufman SL, Zollner P, Blaas D, Allmaier G. 2001. Charge-reduced nano electrospray ionization combined with differential mobility analysis of peptides, proteins, glycoproteins, noncovalent protein complexes and viruses. J Mass Spectrom 36:1038–1052.
11. Kaufman SL, Skogen JW, Dorman FD, Zarrin F, Lewis KC. 1996. Macromolecule analysis based on electrophoretic mobility in air: Globular proteins. Anal Chem 68:1895–1904.
12. Kaufman SL. 1998. Analysis of biomolecules using electrospray and nanoparticle methods: The gas-phase electrophoretic mobility molecular analyzer (GEMMA). J Aerosol Sci 29:537–552.
13. Pease LF, Elliott JT, Tsai DH, Zachariah MR, Tarlov MJ. 2008. Determination of protein aggregation with differential mobility analysis: Application to IgG antibody. Biotechnol Bioeng 101:1214–1222.
14. Pease LF, Sorci M, Guha S, Tsai DH, Zachariah MR, Tarlov MJ, Belfort G. 2010. Probing the nucleus model for oligomer formation during insulin amyloid fibrillogenesis. Biophys J 99:3979–3985.
15. Tsai DH, Zangmeister RA, Pease LF, Tarlov MJ, Zachariah MR. 2008. Gas-phase ion-mobility characterization of SAM-functionalized Au nanoparticles. Langmuir 24:8483–8490.
16. Tsai DH, Pease LF, Zangmeister RA, Tarlov MJ, Zachariah MR. 2009. Aggregation kinetics of colloidal particles measured by gas-phase differential mobility analysis. Langmuir 25:140–146.
17. TSI Inc., Shoreview, MN 2002. Model 3025A ultrafine condensation particle counter. TSI Inc.
18. Hogan CJ, Kettleson EM, Ramaswami B, Chen DR, Biswas P. 2006. Charge reduced electrospray size spectrometry of mega- and gigadalton complexes: Whole viruses and virus fragments. Anal Chem 78:844–852.
19. Lewis KC, Dohmeler DM, Jorgenson JW, Kaufman SL, Zarrin F, Dorman FD. 1994. Electrospray–condensation particle counter: A molecule-counting LC detector for macromolecules. Anal Chem 66:2285–2292.
20. Guha S, Pease LF, Brorson KA, Tarlov MJ, Zachariah MR. 2011. Evaluation of electrospray differential mobility analysis for virus particle analysis: Potential applications in biomanufacturing. J Virol Methods 178:201–208.

21. Li MD, Guha S, Zangmeister RA, Tarlov MJ, Zachariah MR. 2011. Quantification and compensation of nonspecific analyte aggregation in electrospray sampling. Aerosol Sci Technol 45:849–860.
22. Bee JS, Davis M, Freund E, Carpenter JF, Randolph TW. 2010. Aggregation of a monoclonal antibody induced by adsorption to stainless steel. Biotechnol Bioeng 105:121–129.
23. Bolli R, Woodtli K, Bartschi M, Hofferer L, Lerch P. 2010. L-Proline reduces IgG dimer content and enhances the stability of intravenous immunoglobulin (IVIG) solutions. Biologicals 38:150–157.
24. Chen DR, Pui DYH, Kaufman SL. 1995. Electrospraying of conducting liquids for monodisperse aerosol generation in the 4 Nm to 1.8 Mu-M diameter range. J Aerosol Sci 26:963–977.
25. Weidensohler A. 1988. An approximation of the bipolar charge distribution for particles in the submicron size range. J Aerosol Sci 19:387–389.
26. Kim SH, Woo KS, Liu BYH, Zachariah MR. 2005. Method of measuring charge distribution of nanosized aerosols. J Colloid Interface Sci 282:46–57.
27. Knutson EO, Whitby KT. 1975. Aerosol classification by electrical mobility: Apparatus, theory, and applications. J Aerosol Sci 6:443–451.
28. Cech BC, Enke CG. 2000. Relating electrospray ionization response to nonpolar character of small peptides. Anal Chem 72:2723–2723.
29. Li MD, Guha S, Zangmeister RA, Tarlov MJ, Zachariah MR. 2011. Method for determining absolute number concentration of nanoparticles from electrospray sources. Langmuir 27:14732–14739.
30. Guha S, Wayment JR, Li MD, Tarlov MJ, Zachariah MR. 2011. Characterizing the adsorption of proteins on glass capillary surfaces using electrospray–differential mobility analysis (ES–DMA). Langmuir 27:13008–13014.
31. Guha S, Wayment JR, Li MD, Tarlov MJ, Zachariah MR. Protein adsorption on electrospray capillary walls—Influence on aggregate distribution. Journal of Colloids and Interface Science (under review).
32. Laschober C, Kaddis CS, Reischl GP, Loo JA, Allmaier G, Szymanski WW. 2007. Comparison of various nano-differential mobility analysers (nDMAs) applying globular proteins. J Exp Nanosci 2:291–301.
33. Gabrielson JP, Brader ML, Pekar AH, Mathis KB, Winter G, Carpenter JF, Randoplh TW. 2007. Quantitation of aggregate levels in a recombinant humanized monoclonal antibody formulation by size-exclusion chromatography, asymmetrical flow field flow fractionation, and sedimentation velocity. J Pharm Sci 96:268–279.
34. Fukumoto LR, Skura BJ, Nakai S. 1994. Stability of membrane-sterilized bovine immunoglobulins aseptically added to UHT milk. J Food Sci 59:757–759.
35. Lichan E, Kummer A, Losso JN, Kitts DD, Nakai S. 1995. Stability of bovine immunoglobulins to thermal-treatment and processing. Food Res Int 28:9–16.
36. Cao JS, Wang XQ, Zheng HN. 2007. Comparative studies on thermoresistance of protein G-binding region and antigen determinant region of immunoglobulin G in acidic colostral whey. Food Agric Immunol 18:17–30.
37. Law AJR, Banks JM, Horne DS, Leaver J, West IG. 1994. Denaturation of the whey proteins in heated milk and their incorporation into cheddar cheese. Milchwissenschaft Milk Sci Int 49:63–67.
38. Dominguez E, Perez MD, Calvo M. 1997. Effect of heat treatment on the antigen-binding activity of anti-peroxidase immunoglobulins in bovine colostrum. J Dairy Sci 80:3182–3187.
39. Resmini P, Pellegrino R, Hogenboom JA, Andreini R. 1989. Thermal denaturation of whey protein in pasteurized milk. Ital J Food Sci 1:51–62.
40. Lucisano M, Pompei C, Casiraghi E, Rizzo AM. 1995. Milk pasteurization—Evaluation of thermal-damage. Industrie Alimentari 6:185–197.
41. Indyk HE, Williams JW, Patel HA. 2008. Analysis of denaturation of bovine IgG by heat and high pressure using an optical biosensor. Int Dairy J 18:359–366.
42. Roberts CJ. 2003. Kinetics of irreversible protein aggregation: Analysis of extended Lumry–Eyring models and implications for predicting protein shelf life. J Phys Chem B 107:1194–1207.
43. Hartmann WK, Saptharishi N, Yang XY, Mitra G, Soman G. 2004. Characterization and analysis of thermal denaturation of antibodies by size exclusion high-performance liquid chromatography with quadruple detection. Anal Biochem 325:227–239.
44. Mainer G, Sanchez L, Ena JM, Calvo M. 1997. Kinetic and thermodynamic parameters for heat denaturation of bovine milk IgG, IgA and IgM. J Food Sci 62:1034–1038.
45. Kapellios EA, Karamanou S, Sardis MF, Aivaliotis M, Economou A, Pergantis SA. 2011. Using nanoelectrospray ion mobility spectrometry (GEMMA) to determine the size and relative molecular mass of proteins and protein assemblies: A comparison with MALLS and QELS. Anal Bioanal Chem 399:2421–2433.